Strain-tunable Josephson current in graphene-superconductor junction

Y. Wang, Y. Liu, and B. Wang'

Citation: Appl. Phys. Lett. **103**, 182603 (2013); doi: 10.1063/1.4828567
View online: http://dx.doi.org/10.1063/1.4828567
View Table of Contents: http://aip.scitation.org/toc/apl/103/18
Published by the American Institute of Physics

APPLIED PHYSICS LETTERS **103**, 182603 (2013)

Strain-tunable Josephson current in graphene-superconductor junction

Y. Wang,[1] Y. Liu,[2] and B. Wang[1,a)]
[1]*School of Physics and Engineering, Sun Yat-sen University, 510275 Guangzhou, China*
[2]*School of Engineering, Sun Yat-sen University, 510275 Guangzhou, China*

(Received 10 September 2013; accepted 17 October 2013; published online 31 October 2013)

Strain effects on Josephson current in a graphene-superconductor junction are explored theoretically. It is demonstrated that the supercurrent is an oscillatory function of zigzag direction strain with a strain-dependent oscillating frequency. Interestingly, it is found that the Josephson current under armchair direction strain can be turned on/off with a cutoff strain. In view of the on/off properties of the Josephson current, we propose the strained graphene Josephson junction to be utilized as a supercurrent switch. © *2013 AIP Publishing LLC*.
[http://dx.doi.org/10.1063/1.4828567]

Owing to the interplay of superconductivity and the unique electronic structure of graphene, graphene-based superconductors have attracted considerable attention in quantum transport and application of superconductor nanoelectronics. As one of these significant applications, the graphene-based superconductor-normal-superconductor nanostructure (SNS, i.e., Josephson junction) has been theoretically investigated[1–8] and experimentally fabricated by depositing two closely spaced superconductor electrodes on graphene,[9–13] where the proximity effects are responsible for the superconductivity of graphene.[1,6,14] The theoretical and experimental results demonstrate that a finite Josephson current (i.e., supercurrent) can flow at zero charge density in the graphene Josephson junction.[1,9] The unusual phenomenon provides a proof of the relativistic Josephson Effect.[1,9] However, the finite supercurrent limits the application of the graphene Josephson junction in controllable superconductor nanoelectronics with a high on/off ration, such as a supercurrent switch. Recent works on the tunability and external influence of supercurrent concern temperature and size effects,[2–4,11,12] gate-controlled potential barriers,[5,13] and proximity-induced exchange field by a ferromagnetic gate.[7]

The electronic structure in graphene-based nanostructures can also be tuned by mechanical strains. Some investigations have shown that reversible and controlled strains in graphene can be realized by using a suitable substrate patterning,[15,16] a uniform planar tension,[17] or atomic force microscope (AFM) tip.[18] Owing to the large elastic deformation of up to 20% for graphene, the strain in graphene has the advantage of high tunability.[19] It is demonstrated that the mechanical strains in graphene can induce the Dirac cone's deformation resulting in anisotropic group velocity[20,21] and K (K′) point displacements introducing a pseudomagnetic field.[21,22] As a result, the anisotropic velocity and the pseudomagnetic field can be used to manipulate the electronic transport in these nanostructures. The aim of this letter is to report the strain effects on the Josephson current through the graphene SNS junction.

In this letter, we propose a robust supercurrent switch based on the graphene Josephson junction under armchair direction strain, which can turn on/off the Josephson current with a cutoff value. We also investigate the effects of zigzag direction strain on the Josephson current. It is found that the Josephson current is an oscillatory function of the zigzag direction strain with a varied oscillating period.

Hamiltonian, wave functions and Josephson current. We consider a strained graphene SNS junction, where uniaxial strain is applied inside the middle region (II) and superconducting electrodes are deposited on left (I) and right (III) regions. Quasiparticles in regions I and III, as the mixture of electrons and holes, are described by the effective Dirac-Bogoliubov-de-Gennes (DBdG) Hamiltonian[23]

$$\mathbf{H}_{I(III)} = \begin{bmatrix} v_f(\vec{\sigma}_x p_x + \vec{\sigma}_y p_y) - E_F & \Delta_{\mathbf{k}} \\ \Delta^{\dagger}{}_{\mathbf{k}} & E_F - v_f(\vec{\sigma}_x p_x + \vec{\sigma}_y p_y) \end{bmatrix}, \tag{1}$$

where $\vec{\sigma}_x$ and $\vec{\sigma}_y$ are Pauli spin matrices, $\Delta_{\mathbf{k}} = \Delta(\gamma)\exp(i\phi_1)$ in region I and $\Delta_{\mathbf{k}} = \Delta(\gamma)\exp(i\phi_2)$ in region III are the complex pair potentials and only have an angular dependence $\gamma = \mathrm{atan}(k_y/k_x)$ with phases ϕ_1 and ϕ_2, respectively, and E_F is the Fermi energy. Taking into account the conservation of k_y and the mean-field conditions for superconductivity ($\Delta(\gamma) \ll E_F$) and using Eq. (1), one can write the wave functions of these particles moving along $\pm x$ directions in the superconducting regions as $\boldsymbol{\psi}^{\pm}_{I(III)}(x,y) = \boldsymbol{\psi}^{\pm}_{I(III)}\exp(ik_y y)$, with $\boldsymbol{\psi}^{\pm}_{I(III)}$ satisfying

$$\begin{aligned} \boldsymbol{\psi}^{\pm}_{Ie} &= (u,\ \pm ue^{\pm i\gamma},\ ve^{-i\phi_1},\ \pm ve^{-i\phi_1}e^{\pm i\gamma})^T e^{\pm ik_x x}, \\ \boldsymbol{\psi}^{\pm}_{Ih} &= (v,\ \pm ve^{\pm i\gamma},\ ue^{-i\phi_1},\ \pm ue^{-i\phi_1}e^{\pm i\gamma})^T e^{\pm ik_x x}, \\ \boldsymbol{\psi}^{\pm}_{IIIe} &= (u,\ \pm ue^{\pm i\gamma},\ ve^{-i\phi_2},\ \pm ve^{-i\phi_2}e^{\pm i\gamma})^T e^{\pm ik_x x}, \\ \boldsymbol{\psi}^{\pm}_{IIIh} &= (v,\ \pm ve^{\pm i\gamma},\ ue^{-i\phi_2},\ \pm ue^{-i\phi_2}e^{\pm i\gamma})^T e^{\pm ik_x x}, \end{aligned} \tag{2}$$

where $\gamma = \sin^{-1}(k_y\hbar v_f/E_F)$ and $k_x = E_F\cos\gamma/\hbar v_f$. The coefficients u and v are

$$\begin{aligned} u &= \sqrt{1/2 + \sqrt{1 - |\Delta(\gamma)|^2/E^2}/2}, \\ v &= \sqrt{1/2 - \sqrt{1 - |\Delta(\gamma)|^2/E^2}/2}. \end{aligned} \tag{3}$$

a)E-mail: wangbiao@mail.sysu.edu.cn.

The strain-dependent Hamiltonian $\mathbf{H}_{II}$ in the region II reads[21]

$$\mathbf{H}_{II} = \hbar v_f U^{\dagger}(\alpha)[\vec{\sigma}_x(1-\lambda_x\varepsilon)q_x + \vec{\sigma}_y(1-\lambda_y\varepsilon)q_y]U(\alpha)\otimes\vec{\sigma}_0, \tag{4}$$

where α is the angle between the strain direction and graphene zigzag direction (labeled by x-direction), $\lambda_x = 2.2$, $\lambda_y = -0.308$, $U(\alpha) = \mathrm{diag}(1, e^{-i\alpha})$ is the unitary matrix, $\vec{\sigma}_0$ is the identity matrix, ε is the magnitude of strain, and $\boldsymbol{q} = (q_x, q_y)^{\mathrm{T}}$ measures the wave vector displacement from the shifted Dirac points $q_D = \pm[\kappa_0\varepsilon(1+\mu)\cos 3\alpha/a_0, -\kappa_0\varepsilon(1+\mu)\sin 3\alpha/a_0]^T$,[21] with $\kappa_0 \approx 1.6$, $\mu = 0.14$ as Poisson's ratio, and $a_0 = 0.142$ nm as the C-C distance. Note that the energy gap is not considered since the magnitude of strain in this work is limited within 20%, where the gap cannot be opened up.[20] Consequently, the wave functions in strained graphene have the form of

$$\begin{aligned}\boldsymbol{\psi}^{\pm}_{IIe} &= (1,\ \pm s e^{\pm i\theta},\ 0,\ 0)^T e^{\pm i q_{ex} x},\\ \boldsymbol{\psi}^{\pm}_{IIh} &= (0,\ 0,\ 1,\ \mp s' e^{\pm i\theta'})^T e^{\mp i q_{hx} x},\end{aligned} \tag{5}$$

where $s = \mathrm{sgn}(E + E_F - V)$, $s' = \mathrm{sgn}(E - E_F + V)$ with the potential V, θ is the angle of electrons, θ' is the angle of holes due to the Andreev reflection,[23] and the longitudinal wave vectors q_{ex} and q_{hx} are given by

$$\begin{aligned}q_{ex} &= (1-\lambda_x\varepsilon)^{-1}\sqrt{(E+E_F-V)^2/\hbar^2 v_f^2 - (1-\lambda_y\varepsilon)^2(k_y - q_{Dy})^2},\\ q_{hx} &= (1-\lambda_x\varepsilon)^{-1}\sqrt{(E-E_F+V)^2/\hbar^2 v_f^2 - (1-\lambda_y\varepsilon)^2(k_y - q_{Dy})^2}.\end{aligned} \tag{6}$$

Considering $|V - E_F| \geq E_F$ for short tunnel barriers and $E < \Delta(\gamma) \ll E_F$ for the subgap states, we have $E + E_F - V \simeq E_F - V$, $\theta \simeq -\theta'$, $s = -s' = \mathrm{sgn}(E_F - V)$, and $q_{ex} \simeq q_{hx} = q_x$.

Since strain induces the deformation of band structure of graphene and leads to unequal group velocities between the strained regions and the superconductor regions, one should rewrite the wave functions in this form of $\boldsymbol{\Phi}^{\pm}_{I(III)} = \boldsymbol{\psi}^{\pm}_{I(III)}$ and $\boldsymbol{\Phi}^{\pm}_{II} = \boldsymbol{\psi}^{\pm}_{II}/\sqrt{(1-\lambda_x\varepsilon)}$. The total wave functions in three regions can be written as

$$\begin{aligned}\boldsymbol{\Phi}_I &= a_1\boldsymbol{\Phi}^-_I + b_1\boldsymbol{\Phi}^+_I,\\ \boldsymbol{\Phi}_{II} &= a\boldsymbol{\Phi}^+_{IIe} + b\boldsymbol{\Phi}^-_{IIe} + c\boldsymbol{\Phi}^+_{IIh} + d\boldsymbol{\Phi}^-_{IIh},\\ \boldsymbol{\Phi}_{III} &= a_2\boldsymbol{\Phi}^+_{III} + b_2\boldsymbol{\Phi}^-_{III}.\end{aligned} \tag{7}$$

To ensure the requirement of continuity equation, these wave functions should be continuous at $x = -w$ and $x = 0$ of barrier boundaries. Therefore, according to the continuity of $\boldsymbol{\Phi}(x)$, one can obtain the energy spectrum of the Andreev bound states

$$\frac{E^2}{\Delta^2(\gamma)} = \frac{\sin^2(q_x w)[(1 - s\xi\sin\gamma)^2 + (\xi - \sin\gamma)^2] + \eta^2\cos^2\gamma\cos^2(q_x w) + \eta^2\cos^2\gamma\cos\phi}{2[(1 - s\xi\sin\gamma)^2\sin^2(q_x w) + \eta^2\cos^2\gamma\cos^2(q_x w)]}, \tag{8}$$

where $\phi = \phi_2 - \phi_1$ is the phase difference between the right and left superconductors, and the coefficients ξ and η are defined as follows:

$$\xi = (1-\lambda_y\varepsilon)(k_y - q_{Dy})\hbar v_f/|E_F - V|, \quad \eta = (1-\lambda_x\varepsilon)q_x\hbar v_f/|E_F - V|. \tag{9}$$

Note that the existent condition of the subgap Andreev-bound states $E_{\pm}$ in Eq. (8) requires that the longitudinal wave vector q_x in strained region should be real. Taking into account all possible trajectories of particles, one can write the Josephson current in graphene SNS junction as $I_J = \frac{4e}{\hbar}\sum_{m=\pm}\int_{-\pi/2}^{\pi/2} d\gamma f(E_m)\cos\gamma dE_m(\phi)/d\phi$,[1] where $f(x) = 1/(e^{x/k_BT} + 1)$ is the Fermi-Dirac distribution function. Using Eq. (8), we can obtain the Josephson current in the strained graphene SNS junction with length L as follows:

$$I_J/I_0 = \int_{-\pi/2}^{\pi/2} d\gamma\left[\frac{\Delta(\gamma)\eta^2\cos^3\gamma\sin\phi\tanh(E_+/2k_BT)}{E[\sin^2(q_x w)(1 - s\xi\sin\gamma)^2 + \eta^2\cos^2\gamma\cos^2(q_x w)]}\right], \tag{10}$$

where $I_0 = e\Delta_0 E_F L/2\hbar^2\pi v_f$. We assume $\Delta(\gamma) = \Delta_0$ for s-wave is constant only inside the superconducting regions and define the critical supercurrent as $I_C = \max(I_J/I_0)$.

Strain effects on Josephson current. Because strain induces anisotropic Fermi velocity[24,25] and a distribution of Fermi velocity has a strong influence on bound states,[25,26] different direction strains will lead to different effects on the Josephson current. Owing to the D_{6h} point group of the graphene lattice, the zigzag direction strain ($\alpha = 0$) is equivalent to the strain along $\alpha = n\pi/3$ directions and the armchair direction strain ($\alpha = \pi/2$) is identical to the strain along $\alpha = (2n+1)\pi/6$ directions, where n is an integer. Therefore, we can only pay attention to the typical zigzag and armchair directions. We first investigate the effect of the zigzag direction strain on the Josephson current in Figs. 1(a) and 1(b). To ensure that the electron density of states agrees well with a true system, some valid values are used: $E_F = 0.1\,\text{eV}$, $V/E_F = 10$, $k_BT = 0.01\Delta_0$, and $w = \lambda_F/\pi$, where $\lambda_F = 2\pi/k_F$ is the Fermi wavelength. From Fig. 1(a), one can observe that the Josephson current is an oscillatory function of the strain magnitude ε. Previous investigations have shown that the Josephson current is an oscillatory function of the gate-controlled potential V with an unvaried oscillating frequency.[5] However, in the presence of the zigzag direction strain, the oscillating frequency increases with enhanced magnitude ε, since the strain-induced group velocity of $v_x = v_f/(1-2.2\varepsilon)$ increases with strengthened ε. The oscillating Josephson current induced by the zigzag direction strain also happens in the Josephson junction of graphene ribbon.[27] On the other hand, due to the periodical characteristics of the oscillating current, we can only consider the current-phase relation inside single period, such as the period of ε from 0.055 to 0.11 with the peak of $\varepsilon_p = 0.085$. The results are plotted in Fig. 1(b). As can be seen, the closer the strain magnitude ε is to ε_p, the more the current-phase relation deviates from the sinusoidal form. The oscillating current with a tunable period and the current-phase relation in a controlled fashion may be applied to strain-engineered superconducting logic circuits.[7] Recently, a phase-sensitive SQUID (superconducting quantum interference device) interferometry technique has been used to directly observe the current-phase relation.[28] It is possible to apply the interferometry technique to examine the strain effects on the current-phase relation.

We further investigate the effects of the armchair direction strain on the Josephson current in Figs. 2(a) and 2(b). To compare with the influence of the zigzag direction strain, we consider the identical values of E_F, w, k_BT, and V/E_F as in Fig. 1(a). The Josephson current as a function of ε is shown in

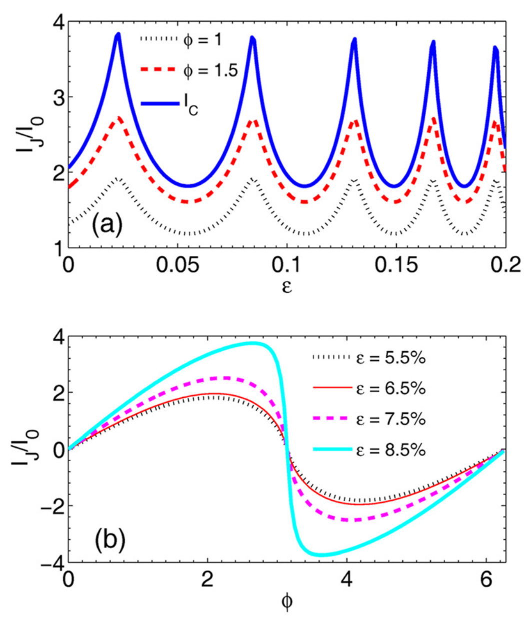

FIG. 1. Effects of zigzag direction strain: (a) Josephson current as a function of the strain magnitude ε and (b) the current-phase relation for $E_F = 0.1\,\text{eV}$, $w = \lambda_F/\pi$, $k_BT = 0.01\Delta_0$, and $V/E_F = 10$.

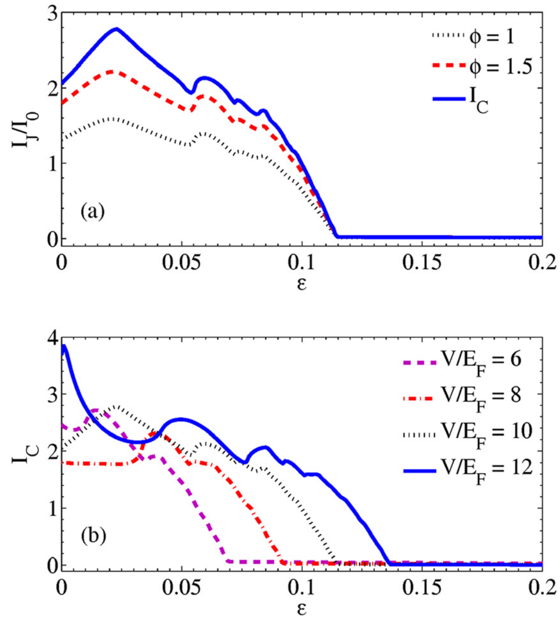

FIG. 2. Effects of armchair direction strain: (a) Josephson current as a function of the strain magnitude ε with $V/E_F = 10$ and (b) critical supercurrent as a function of the strain magnitude ε for $E_F = 0.1\,\text{eV}$, $w = \lambda_F/\pi$, and $k_BT = 0.01\Delta_0$.

Fig. 2(a). With the increased strain magnitude, the currents including the critical current I_C decrease to zero. This means that the armchair direction strain can turn on/off the Josephson current. Physically, the Josephson current is carried by the subgap Andreev bound states, which require the longitudinal wave vector q_x in strained region to be real, i.e., $|E_F - V| \geq |(1-\lambda_y\varepsilon)(k_y - q_{Dy})|$ with $q_{Dy} = -\kappa_0\varepsilon(1+\mu)\sin 3\alpha/a_0$. In other words, if q_x becomes imaginary, the Andreev bound states will not exist and the Josephson current will not be produced. Obviously, for the armchair direction strain, the shifts of Dirac point ($-q_{Dy} \simeq 84.55\varepsilon$) dramatically increase with the enhanced strain and lead to the imaginary q_x. Therefore, we attribute the supercurrent switch effect under the armchair strain to the shift of Dirac point. From Fig. 2(a), one can also observe that the Josephson current has a cutoff strain ε_{off}. Owing to $(1-\lambda_y\varepsilon)(k_y - q_{Dy}) \leq (1-\lambda_y\varepsilon)(k_F - q_{Dy})$, we can obtain an approximate value of the cutoff strain from $|E_F - V| = |(1-\lambda_y\varepsilon)(k_F - q_{Dy})|$ as follows:

$$\varepsilon_{off} = \frac{-a_0k_F\lambda_y + \kappa_0(1+\mu)\sin 3\alpha + \sqrt{\chi}}{2\kappa_0\lambda_y(1+\mu)\sin 3\alpha}, \qquad (11)$$

where $\chi = [\kappa_0(1+\mu)\sin 3\alpha + a_0k_F\lambda_y]^2 + 4a_0\kappa_0k_F\lambda_y(1+\mu)(V/E_F)\sin 3\alpha$. Note that Eq. (11) is valid only under the condition of $q_{Dy} \neq 0$. For $q_{Dy} = 0$ such as the zigzag direction strain, the Dirac point is never shifted and the Josephson current cannot be turned off, as previously demonstrated. Equation (11) also shows that the cutoff strain depends on the potential V and the strain magnitude ε. Therefore, we plot the critical supercurrent as a function of the strain magnitude ε at different potentials in Fig. 2(b). As can be seen, the cutoff strain is tuned by the potential V. In addition, the switch performance is very robust. The good on/off ration and the controllable cutoff values of the Josephson current indicate that the graphene Josephson junction under the

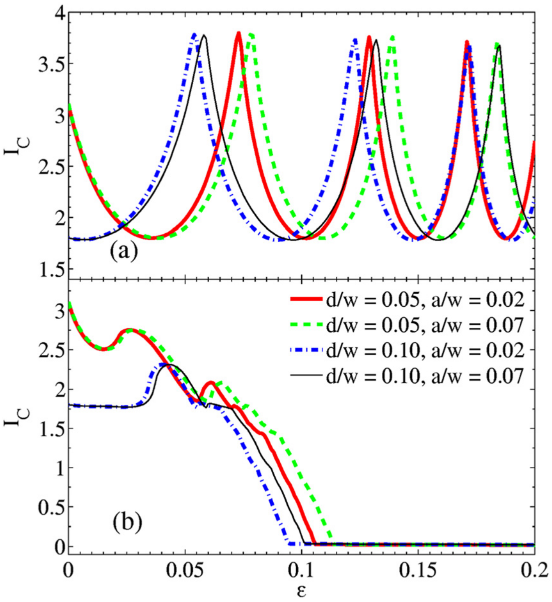

FIG. 3. Critical supercurrent as a function of the strain magnitude ε for the real potential profile $V(x)$ in Eq. (12) and strain profile $\varepsilon(x)$ in Eq. (13), with $E_F = 0.1$ eV, $w = \lambda_F/\pi$, $k_B T = 0.01\Delta_0$, and $V/E_F = 10$; (a) zigzag direction strain and (b) armchair direction strain.

armchair direction strain is a promised candidate of a supercurrent switch.

In real situations, there are always some boundary effects such as the boundary of potential barriers and the strain smoothness at the graphene-superconductor interface. To explore how these interface effects affect the Josephson current, we adopt a typical potential profile[29] and strain profile[21]

$$V(x) = 0.5V[erf(2(x+w)/d - 2) + erf(-2x/d - 2)] \quad (12)$$

and

$$\varepsilon(x) = \frac{\varepsilon}{\tanh(w/4a)}[1/(1+e^{-(x+w)/a}) - 1/(1+e^{-x/a})], \quad (13)$$

where $erf(x)$ is the error function with the smoothing parameters d and a. The numerical results are plotted in Figs. 3(a) and 3(b). Indeed, it is clear that the smoothness of the interfaces has an obvious influence on the Josephson current. However, the oscillating effects of the current and the switch effects of the Josephson current remain in all cases. Therefore, the smoothness of the strain and potential profiles will not restrict the application of the current oscillations and the switch effects of the strained graphene Josephson junction in superconducting electronics.

In summary, we have explored the strain effects on the Josephson current in a graphene SNS junction. It is found that the Josephson current is an oscillatory function of the zigzag direction strain and the oscillating period is varied with the enhanced strain. However, the results in the presence of the armchair direction strain demonstrate that the Josephson current can be turned on/off with a cutoff strain. We attribute the on/off behavior of the current to the strain-induced displacement of Dirac point and propose the graphene Josephson junction under the armchair direction strain as a supercurrent switch.

We are grateful for the support from the National Natural Science Foundation of China (Nos. 10902128, 10732100, and 11072271).

[1] M. Titov and C. W. J. Beenakker, Phys. Rev. B **74**, 041401(R) (2006).
[2] A. G. Moghaddam and M. Zareyan, Phys. Rev. B **74**, 241403(R) (2006).
[3] J. González and E. Perfetto, Phys. Rev. B **76**, 155404 (2007).
[4] I. Hagymási, A. Kormányos, and J. Cserti, Phys. Rev. B **82**, 134516 (2010).
[5] M. Maiti and K. Sengupta, Phys. Rev. B **76**, 054513 (2007).
[6] A. M. Black-Schaffer and S. Doniach, Phys. Rev. B **78**, 024504 (2008).
[7] J. Linder, T. Yokoyama, D. H. Hernando, and A. Sudbø, Phys. Rev. Lett. **100**, 187004 (2008); A. G. Moghaddam and M. Zareyan, Phys. Rev. B **78**, 115413 (2008).
[8] J. Linder, A. M. Black-Schaffer, T. Yokoyama, S. Doniach, and A. Sudbo, Phys. Rev. B **80**, 094522 (2009).
[9] H. B. Heersche, P. Jarillo-Herrero, J. B. Oostinga, L. M. K. Vandersypen, and A. F. Morpurgo, Nature **446**, 56 (2007).
[10] X. Du, I. Skachko, and E. Y. Andrei, Phys. Rev. B **77**, 184507 (2008).
[11] U. C. Coskun, M. Brenner, T. Hymel, V. Vakaryuk, A. Levchenko, and A. Bezryadin, Phys. Rev. Lett. **108**, 097003 (2012).
[12] I. V. Borzenets, U. C. Coskun, S. J. Jones, and G. Finkelstein, Phys. Rev. Lett. **107**, 137005 (2011).
[13] G. H. Lee, D. Jeong, J. H. Choi, Y. J. Doh, and H. J. Lee, Phys. Rev. Lett. **107**, 146605 (2011).
[14] A. Shailos, W. Nativel, A. Kasumov, C. Collet, M. Ferrier, S. Guéron, R. Deblock, and H. Bouchiat, EPL **79**, 57008 (2007).
[15] Z. H. Ni, T. Yu, Y. H. Lu, Y. Y. Wang, Y. P. Feng, and Z. X. Shen, ACS Nano **2**, 2301 (2008).
[16] V. M. Pereira and A. H. C. Neto, Phys. Rev. Lett. **103**, 046801 (2009).
[17] V. M. Pereira, A. H. C. Neto, and N. M. R. Peres, Phys. Rev. B **80**, 045401 (2009).
[18] C. Lee, X. Wei, J. W. Kysar, and J. Hone, Science **321**, 385 (2008).
[19] K. S. Kim, Y. Zhao, H. Jang, S. Y. Lee, J. M. Kim, K. S. Kim, J. H. Ahn, P. Kim, J. Choi, and B. H. Hong, Nature **457**, 706 (2009).
[20] S. M. Choi, S. H. Jhi, and Y. W. Son, Phys. Rev. B **81**, 081407(R) (2010).
[21] F. M. D. Pellegrino, G. G. N. Angilella, and R. Pucci, Phys. Rev. B **84**, 195404 (2011).
[22] F. Guinea, M. I. Katsnelson, and A. K. Geim, Nat. Phys. **6**, 30 (2010).
[23] C. W. J. Beenakker, Phys. Rev. Lett. **97**, 067007 (2006).
[24] F. M. D. Pellegrino, G. G. N. Angilella, and R. Pucci, Phys. Rev. B **85**, 195409 (2012).
[25] Y. Wang, Y. Liu, and B. Wang, Appl. Phys. Express **6**, 065102 (2013).
[26] Y. Wang, Y. Liu, and B. Wang, Physica E **48**, 191 (2013); **53**, 186 (2013).
[27] J. Zou and G. Jin, Appl. Phys. Lett. **98**, 122106 (2011).
[28] C. D. English, D. R. Hamilton, C. Chialvo, I. C. Moraru, N. Mason, and D. J. Van Harlingen, e-print arXiv: 1305.0327.
[29] F. Zhai, Y. Ma, and K. Chang, New J. Phys. **13**, 083029 (2011).